CHAPTER 5
Protein Folding Under Crowded Conditions

5.1 INTRODUCTION

5.1.2 Environment and Protein Folding

In the past few decades, understanding the way in which proteins are encoded to fold to a specific three dimensional structure has emerged as a vibrant area of scientific research.[1-9,12] While the knowledge base of protein folding has increased dramatically, little of this work directly focuses on the environment of proteins as they fold *in vivo*.[19] In fact, the established connection between environment and protein misfolding, which is implicated in many diseases, demonstrates the importance of investigating environmental effects.[10,11,33,34,38]

5.1.3 Cytoplasm Environment

Cytoplasm, the native environment of proteins, is by all accounts a very complex stew. Between five and 40 % of cytoplasm volume is occupied by macromolecules, such as proteins, sugars, and structural fibers. These macromolecules create extremely confined microenvironments that often have much higher viscosities than water alone. However, there is much debate regarding the description of the microenvironment organization, ranging from "lattice-like mesh" to "liquid crystal structure".[13-16] Data suggest that the cytoplasm is composed of a solid and fluid phase, in which the latter phase has a viscosity ~1.3 times that of water.[15] The solid phase of cytoplasm is typically comprised of

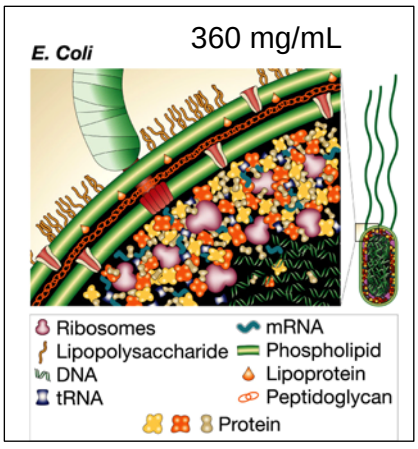

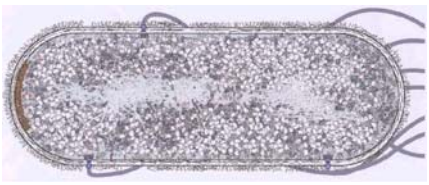

Figure 5.1. Representation of the crowded interior of the cell (top) and image of crowded bacteria (bottom).[17,18]

structural networks made from actin and/or membranes.[42] A protein diffusing through cytoplasm is not only slowed by higher liquid viscosity, but also by collisions with mechanical barriers and perhaps nonspecific binding to other macromolecules.[15,26,30,38] The effective viscosity encountered by such a protein is actually 2-5 times higher than that of water.[16] Yet the *E. coli* lac repressor finds and binds to an operator site on DNA at up to 1000 times faster than the expected diffusion rate, due to "metabolite channeling" which passes a substrate directly from one location to another, bypassing the crowded conditions of the cytoplasm.[17] Experimentalists have observed under crowded conditions both stabilized native states[27] and destabilized native states[37], faster folding rates[27] and changes in folding mechanisms.[34] Thus both function and folding of proteins are strongly influenced by the crowded cellular environment. However, most *in vitro* studies do not account for these interactions, which is a considerable oversight when trying to understand biological processes.

5.1.4 Crowding Theory

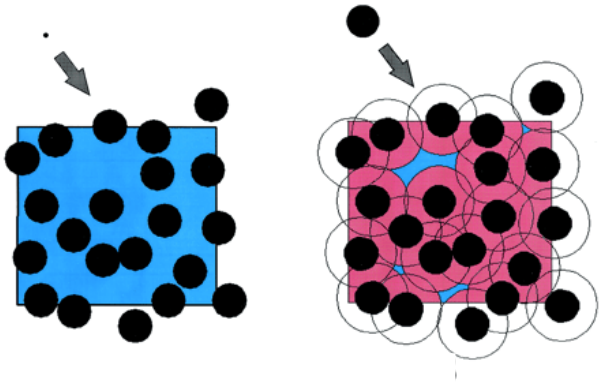

Figure 5.2. The square represents a volume in which 30% of the available space is occupied by macromolecules. A small molecule (left) has access to the remaining 70% of the volume while a molecule of approximately the same size (right) is excluded from much of the volume.[20]

The crowded conditions found in cytoplasm change the thermodynamics and kinetics of processes in the cell. Generally, proteins under crowded conditions thermodynamically favor compaction of macromolecules, whether to give greater structure to a protein than found under dilute conditions or to form

non-native amyloid fibers.[17,20] Crowding can either increase or decrease kinetics of biochemical processes. Some evidence shows crowding causes the formation of more compact structures in certain enzymes resulting in higher rates of reactivity.[21] Indeed, the thermodynamics and kinetics might differ by orders of magnitude in crowded conditions from dilute solutions. However, few experimentalists have probed the rates of protein folding under crowded conditions.

The main interaction of macromolecules under crowded conditions is nonspecific steric repulsion, resulting in a dramatic decrease in the available volume of the solution, often called the excluded volume effect. In crowded solutions, the volume available to a specific macromolecule depends on its size and the size and concentration of the surrounding macromolecules. A smaller molecule has much greater access and mobility than a larger molecule, just as motorcycles weave through stopped traffic much easier than limousines.

5.1.5 Techniques and Previous Work

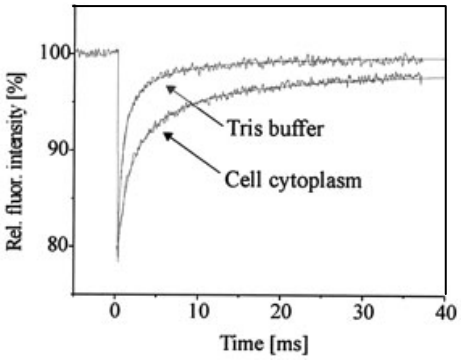

Figure 5.3. Fluorescence recovery of GFP in cell cytoplasm (D = 87 $\mu m^2/s$) and tris buffer (D = 24 $\mu m^2/s$).[14]

One technique often used to study crowded solutions is fluorescence recovery after photobleaching (FRAP). Simply, a macromolecule labeled with a fluorophore is excited to the point of photobleaching and a weaker probe is used to monitor when non-bleached macromolecules have diffused into the bleached space. FRAP results have shown that diffusion in crowded solutions is substrate

dependent. The diffusion rate of DNA and dextran (poly D-glucose with few branches) appears to be dependent on substrate size, as smaller macromolecules diffuse at greater speeds. Ficoll, a highly-branched polymer of sucrose and epichlorohydrin, has size-dependent diffusion in cytoplasm as well. However, after a certain size (particle radius = 140 Å) the more rigid Ficoll becomes effectively immobilized.[14] The goal of the research in this report is to apply the knowledge that macromolecules behave differently in crowded conditions to the problem of protein folding.

5.2 RESULTS AND DISCUSSION

5.2.2 Thermodynamic Results

The choice of crowding agent for protein folding experiments under crowded conditions is not obvious. Ellis outlines the desiratum for a crowding agent, many of which are difficult, if not impossible to achieve: the crowding agent must be water soluble, can not affect the pH, ionic strength or have any specific interactions with not only the protein being crowded, but also itself.

Common crowding agents are hemoglobin, bovine serum albumin (BSA), vesicles, dextran, ficoll, polyvinyl alcohol, and polyethylene glycol.[20-22] Since cyt *c* was initially used in an unlabeled form, and fluorescence of the native tryptophan-59 was measured under crowded conditions, the crowding agent could not contain tryptophan as well. This eliminated the crowding agents bovine serum albumin (BSA) and human serum albumin (HSA), as they were highly fluorescent. Initially, small unilamilar vesicles (SUVs) were used to crowd h-cyt *c*, however SUVs were found to interact specifically with h-cyt *c*[23]. Polyethylene glycol (MW=8000) was chosen as a crowding agent since its molecular weight is in the range of cyt *c* (MW=12384), it is highly soluble, and has very

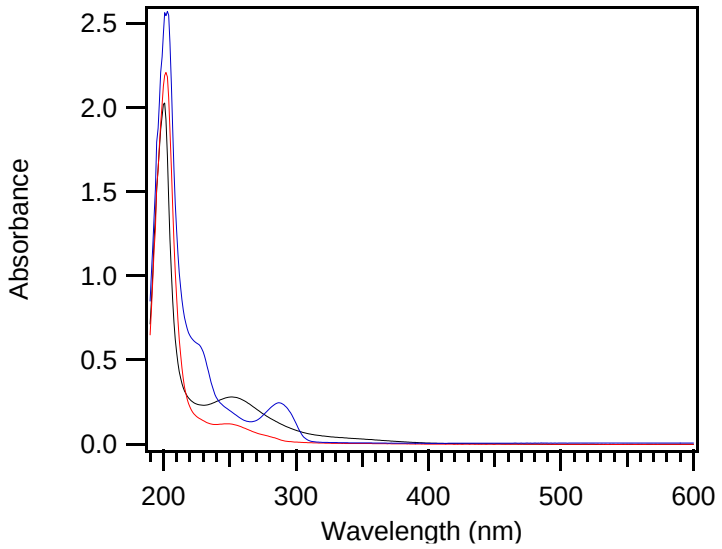

Figure 5.4. Absorption spectra of 100 mg/mL solutions of common crowding agents: 8000 MW PEG (red), 35000 MW PEG (blue), Ficoll (black).

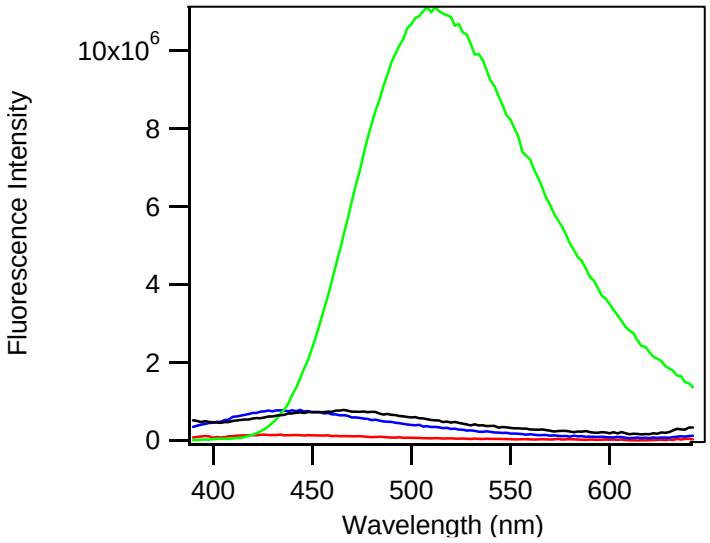

Figure 5.5. Steady-state fluorescence spectra of 100 mg/mL solutions of common crowding agents excited at 355 nm: 8000 MW PEG (red), 35000 MW PEG (blue), Ficoll (black), 20 μM Dansyl model (green).

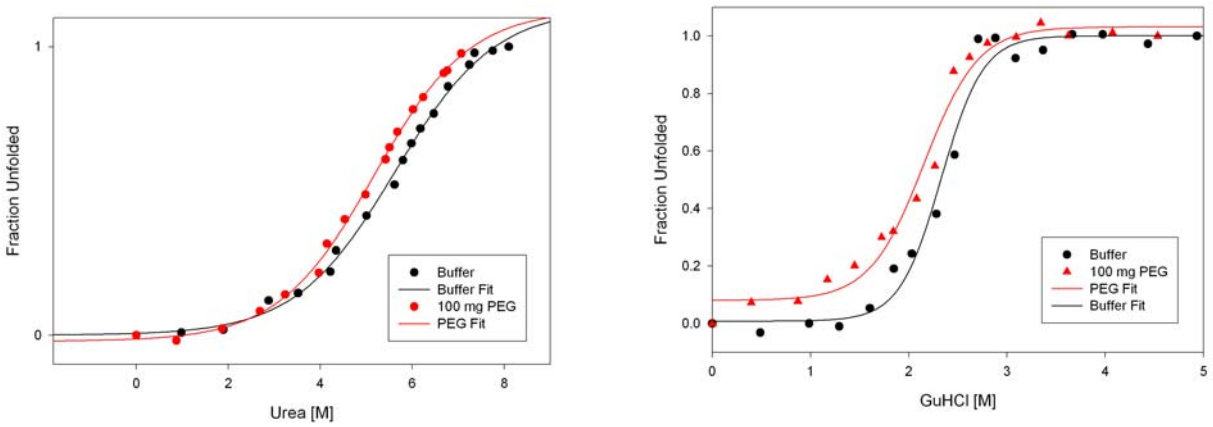

Figure 5.6. Equilibrium titration curve of h-cyt c in urea (left) and GdmCl (right) in buffer and with 100 mg 8000 MW PEG as a crowding agent.

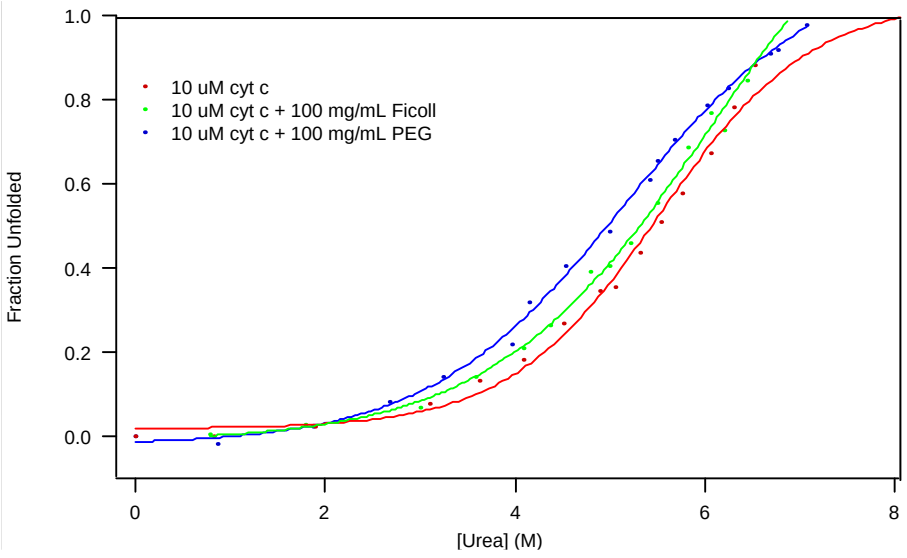

Figure 5.7. Equilibrium urea unfolding curve of DNS(C102)-cyt *c* in the presence of 100 mg/mL Ficoll and 8000 MW PEG crowding agents.

little fluorescence. Higher molecular weight polyethylene glycols (PEGs) were considered, and some experiments were conducted with 35,000 MW PEG, however solubility became an issue at higher denaturant concentrations. In addition, the 35,000 MW PEG samples were noticably more viscous than the 8000 MW PEG samples. Although viscosity is higher in the cytoplasm, it is desirable to decouple this effect from excluded volume considerations. Ficoll, a high molecular weight polysaccharide with a radii range from 2-7 nm, close to the 6 nm radius of cyt *c* obtained from DLS, was also used as a crowding agent due to its high solubility and low viscosity[24, 25]. Note that there is no background in the circular dichroism spectra of Ficoll, 8000 MW PEG and 35000 MW PEG. Ficoll (λ_{max}=470 nm) and 35000 MW PEG (λ_{max}=445 nm) have small fluorescence emission profiles with 355 nm excitation, however this can be decoupled from the fluorescence decays obtained through FET kinetics experiments (Figure 5.14).

Titration curves of h-cyt *c* in the presence of crowding agent show slight destabilization in both urea and GdmCl (Figure 5.6). The behavior under crowded conditions was reproduced for DNS-labeled yeast cyt *c* in urea unfolding curves; Figure 5.16 illustrates the slight destabilization in PEG and Ficoll solutions. The CD temperature unfolding curve of the DNS(C102)-cyt *c* also shows slight stabilization in Ficoll solution at pH 4.28 (Figure 5.7). There is no discernable difference in the CD spectra of folded DNS(C102)-cyt *c* under the same conditions (Figure 5.9). However, fluorescence guanidine unfolding curves shows little difference in midpoints between Ficoll (100 and 200 mg/mL) and 50 mM NaOAc, ph 4.28 solutions of DNS(C102)-cyt *c* (Figures 5.8 and 5.10). Although small, the difference in the midpoints of cyt *c* under crowded conditions led to the obvious question of how crowding agent affects the denatured

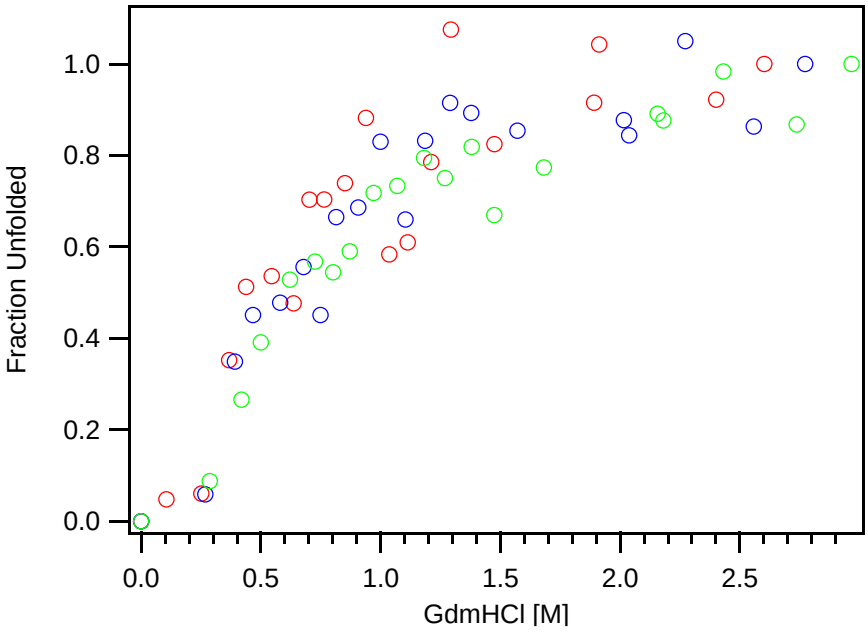

Figure 5.8. Circular dichroism of folded DNS(C102)-cyt *c* in 50 mM NaOAC buffer, pH 4.28 (red) and in the presence of 100 mg/mL (blue) and 200 mg/mL (green) Ficoll crowding agent, also 50 mM NaOAC, pH 4.28.

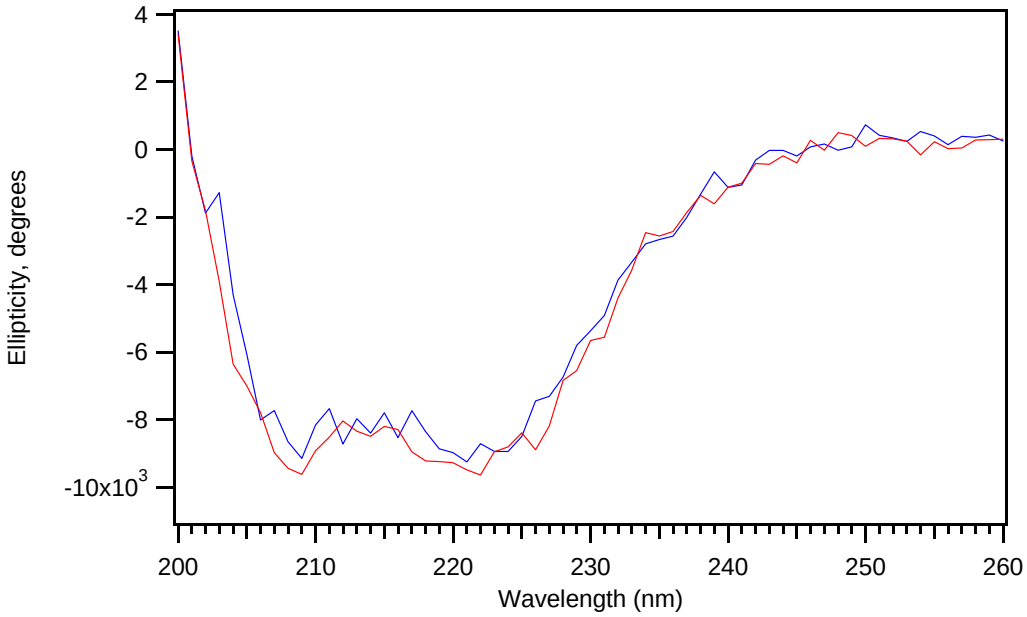

Figure 5.9. Circular dichroism of folded DNS(C102)-cyt *c* in 50 mM NaOAC buffer, pH 4.28 (red) and in the presence of 100 mg/mL Ficoll crowding agent at pH 4.28 (blue).

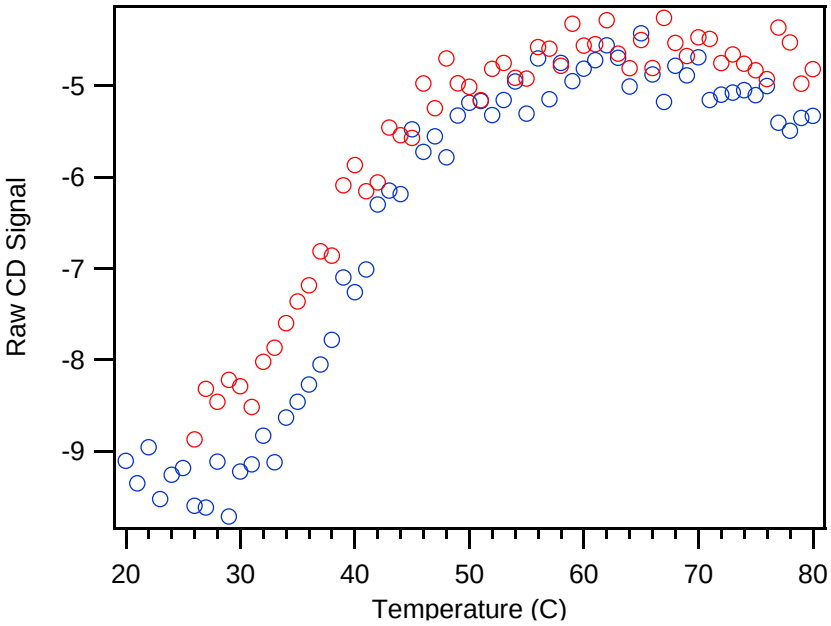

Figure 5.10. Circular dichroism temperature unfolding curve of DNS(C102)-cyt *c* in 50 mM NaOAC buffer, pH 4.28 (red) and in the presence of 100 mg/mL Ficoll crowding agent at pH 4.28 (blue).

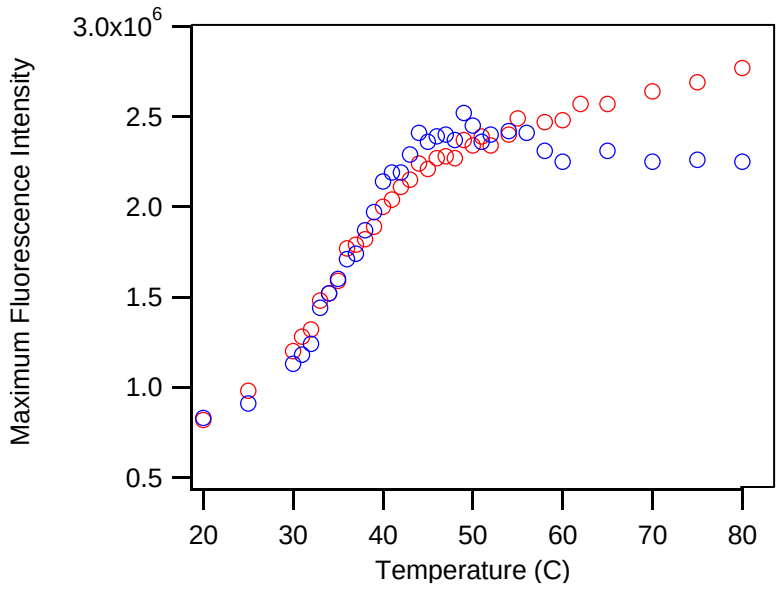

Figure 5.11. Maximum fluorescence at various temperatures. of DNS(C102)-cyt *c* in 50 mM NaOAC buffer, pH 4.28 (red) and in the presence of 100 mg/mL Ficoll crowding agent at pH 4.28 (blue).

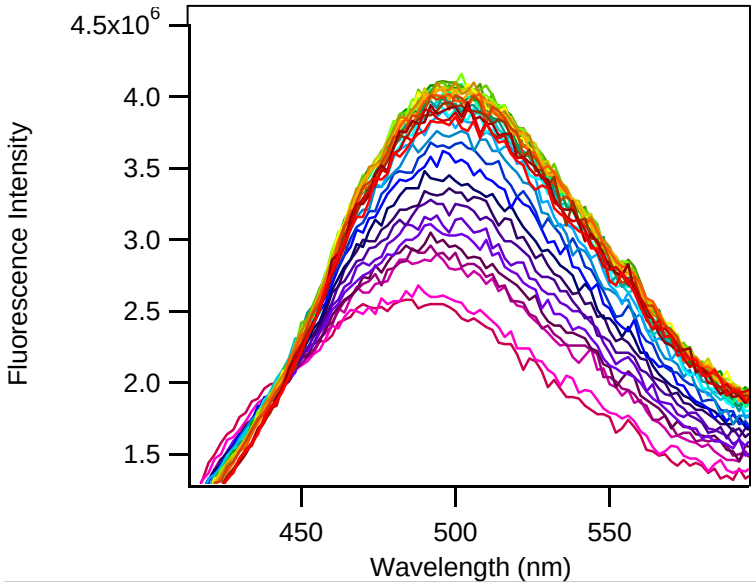

Figure 5.12. Fluorescence temperature titration of DNS(C102)-cyt *c* in the presence of 100 mg/mL Ficoll crowding agent in 50 mM NaOAc buffer at pH 4.28.

protein structure. Is the unfolded h-cyt *c* in a non-native more compact form, as predicted by theory, or more extended than in dilute solutions? FRET experiments which determine the distance between the heme and the tryptophan in h-cyt *c*, and therefore provide a description of the extended structures, were initiated.

5.2.3 FET Kinetics

The fluorescence decay kinetics of h-cyt *c* were collected under crowded conditions (100 mg/mL of 8000 MW PEG). As expected, excitation of W59 by the third harmonic (290 nm) of a Ti:sapphire laser was quenched by the heme in the folded state by the heme and less quenched in the unfolded states. The distribution of extracted rate constants demonstrates only small differences in the crowded solutions; in buffer and both denaturants, the crowded solutions exhibit slower decays, possibly indicating a more extended structure (Figure 5.13). These results would concur with the data from the equilibrium steady-state titration curves, however factors such as the viscosity and refractive index might also affect the rate constants.

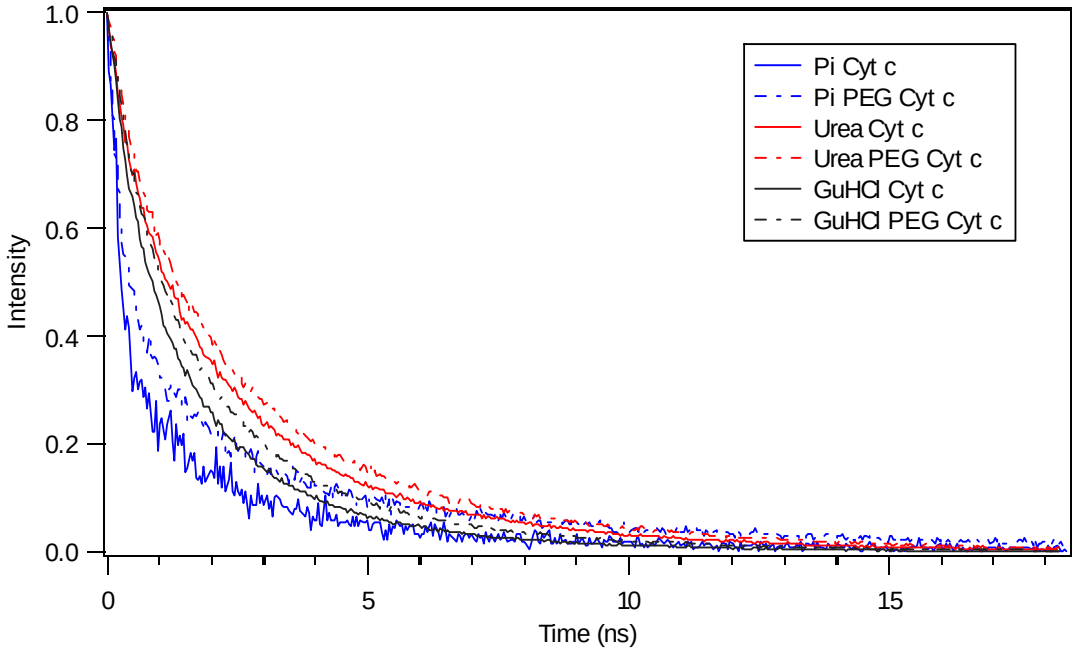

Figure 5.13. Fluorescence decays of h-cyt c in 20 mM NaPi, pH 7.0 (blue), ~9 M urea (red), and ~5 M GdmCl (black) in dilute solution (solid) and under crowded conditions (100 mg/mL of 8000 MW PEG (dashed)).

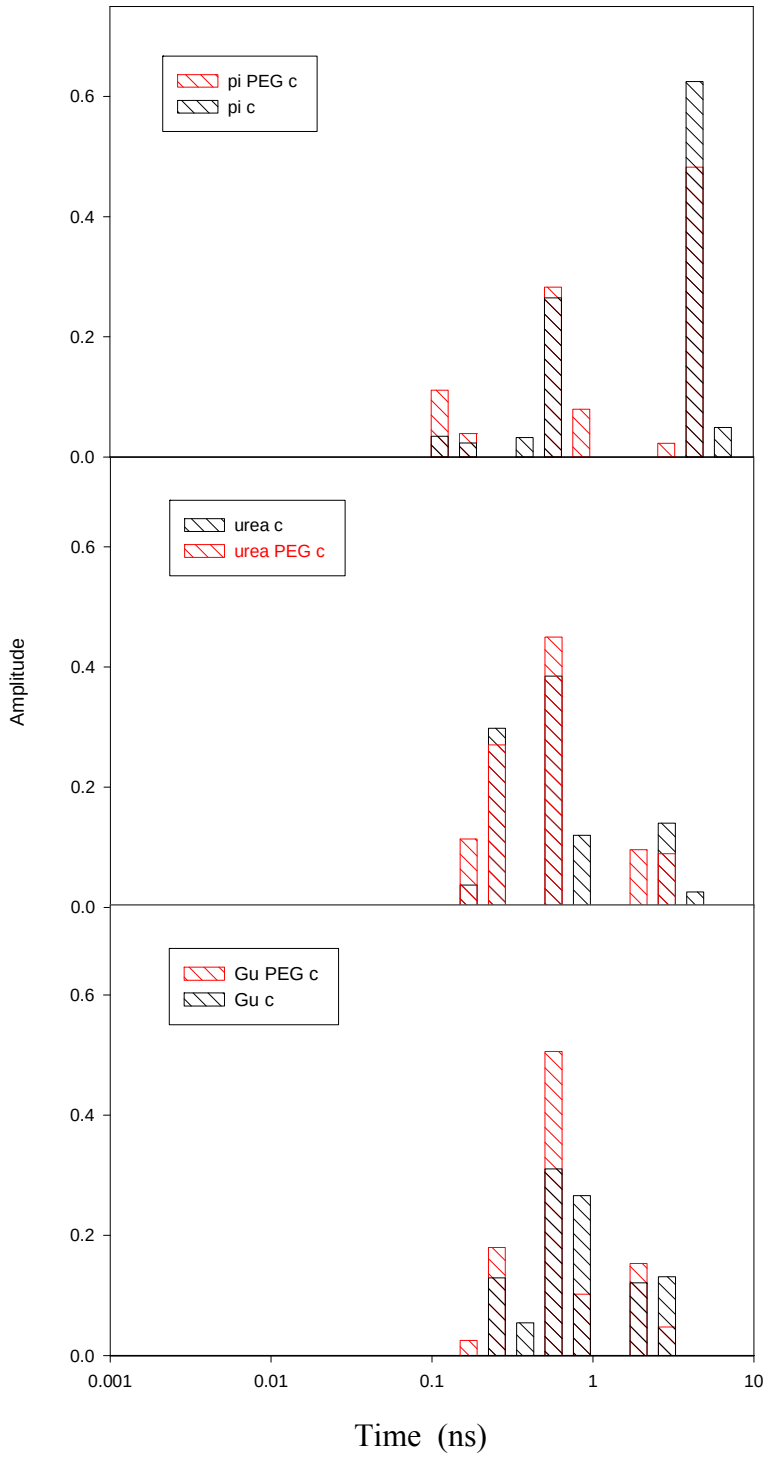

Figure 5.14. Extracted rate constants from fluorescence decays of h-cyt c in 20 mM NaPi, pH 7.0 (top), ~9 M urea (middle), and ~5 M GdmCl (bottom) in dilute solution (black) and under crowded conditions (100 mg/mL of 8000 MW PEG (red)).

5.3 CONCLUSIONS

Under equilibrium conditions, both h-cyt *c* and DNS(C102)-cyt *c* show slight destabilization in crowded solutions. The FET kinetics indicate the unfolded states might be more extended under crowded conditions. However, the observed differences are small and not significant when the complicating factors such as change in viscosity are considered. Future work should focus rather on the effect of crowding agents on the rate of cyt *c* folding. Using a stopped-flow mixer, the rapid dilution of crowded, denatured cyt *c* would initiate the refolding of the protein. Since the folding rates of cyt *c* have been studied extensively, any crowding effect should be easy to determine.

5.4 METHODS AND MATERIALS

5.4.2 Purification of Horse Heart Cytochrome *c* and *Saccharomyces cerevisiae* iso-1 cytochrome *c*

The proteins were purchased from Sigma, dissolved in 20 mM NaPi, pH 7.0 and oxidized with ferricyanide (Sigma-Aldrich). The oxidizer was separated from the protein using gel filtration (PD-10; GE Healthcare, Piscataway, NJ). The oxidized protein was further purified using an Akta FPLC system equipped with an ion-exchange column (Mono S; HR 10/10, Pharmacia, New York, NY).

5.4.3 Labeling of *Saccharomyces cerevisiae* iso-1 cytochrome *c*

Saccharomyces cerevisiae iso-1 cytochrome *c* (Sigma, St. Louis, MO) was dissolved in 100 mM NaPi, pH 7.4 and stirred under argon. The protein was denatured with 3 M of urea. The DNS fluorophore, 5-((((2-iodoacetyl)amino)ethyl)amino) naphthalene-1-sulfonic acid (1,5-I-AEDANS; Invitrogen Molecular Probes, Carlsbad, CA), was dissolved in 1 mL of dimethyl sulfoxide (DMSO) and delivered dropwise into

the protein solution. The labeling reaction at the sulfhydryl C102 group was allowed to proceed under argon in the dark for three hours.

5.4.4 Purification and Characterization of Dansyl-labeled *Saccharomyces cerevisiae* iso-1 cytochrome *c*

The excess DNS was removed from the protein by gel filtration (PD-10; GE Healthcare, Piscataway, NJ). The labeled protein was further purified using an Akta FPLC system equipped with an ion-exchange column (Mono S; HR 10/10, Pharmacia, New York, NY) and repurified after a week.

5.4.5 Buffer and Sample Preparation

The solutions for the equilibrium unfolding curves of cyt *c* under crowded conditions were prepared from a concentrated GdmCl solution, which was diluted to nearly twenty concentrations. Each were individually corrected for changes in pH. To 1.0 mL of these solutions, 100 milligrams of 8000 MW PEG were added and vortexed until dissolved. An average increase in volume of 7 % was observed and the protein concentration was corrected accordingly. Similar steps were taken for the urea samples, without the pH correction.

Typical protein sample concentrations were 1 to 10 μM and were prepared by diluting small amounts of a concentrated stock solution into 1 mL of sample solution. Buffers used were 20 mM NaPi at pH 7.0, 5 mM NaOAc at pH 4.28, and 0.8 M and 3 M GdmCl (adjusted to pH 7 if 20 mM NaPi or pH 4.28 if 5 mM NaOAc). All samples were protected from light and prepared for laser data collection by evacuating all gas from a septum-sealed cuvette and refilling with argon gas. This pump/purge procedure was typically repeated three times.

5.4.6 Steady-state Equilibrium Experiments

Absorption spectra were recorded on a Hewlett-Packard 8453 diode-array spectrophotometer (Santa Clara, CA). Protein concentrations were estimated by using ε_{410} = 106 000 M^{-1} cm^{-1} for oxidized, folded, Fe(III) DNS(C102)-cyt *c*. Circular dichroism data were acquired using an Aviv Model 62ADS spectropolarimeter (Aviv Associates, Lakewood, NJ) equipped with a thermostated sample holder. Scans were recorded from 210 to 260 nm at 1-nm intervals with an integration time of 5 s and a bandwidth of 1.5 nm. Spectra were collected at 20 °C and in a 1-mm fused-silica cuvette unless otherwise specified. The thermal unfolding curve was generated from the ellipticity at 222 nm, recorded from 20 °C to 80 °C at 1 °C intervals. All spectra were background subtracted.

Steady-state fluorescence measurements were performed with a Jobin Yvon/SPEX Fluorolog spectrofluorometer (HORIBA Jobin Yvon, Model FL3-11, Edison, NJ) equipped with a Hamamatsu R928 PMT (Hamamatsu Photonics, Bridgewater, NJ). Samples (~1 μM) were excited at 355 nm (2-nm band-pass) and luminescence was observed from 420 to 650 nm at 1-nm intervals with 0.5 s integration times at room temperature or as otherwise specified. Background spectra of buffer only were also recorded and subtracted from DNS(C102)-cyt *c* spectra.

5.4.7 Fluorescence Energy Transfer Kinetics

The third harmonic of a femtosecond Ti:Sapphire regenerative amplifier (Spectra-Physics) was used to excite tryptophan at a 1 kHz repetition rate with 292 nm light. The time resolution of the laser, determined by the full width at half maximum (FWHM) of the instrument response function, is 300 ps. Excitation power at the sample was ~550-650 μW and a 355 ± 5nm (or 325 ± 5nm) filter was used to select for tryptophan emission. A

UG11 glass filter was used that allows passage of only ultravisible light below 400nm. Emission was transferred using an optical fiber connected to a picosecond streak camera (Hamamatsu C5680) in photon-counting mode. Measurements were recorded under magic angle polarization conditions (O'Connor & Phillips, 1984) and emission was detected at 90^{o} to the excitation beam. Minimal photobleaching (< 10%) was confirmed by recording UV-visible absorption spectra before and after laser measurements.

Fluorescence decay measurements of DNS(C102)-cyt *c* were performed using the third harmonic of a regeneratively amplified Nd-YAG laser (355 nm, 50 ps, <0.5 mJ) for fluorophore excitation and a picosecond streak camera (Hamamatsu C5680) in photon counting mode for detection. Magic-angle polarization was used for both excitation and collection. DNS fluorescence was selected with a 420-nm long-pass cutoff filter.

Temperature was measured with a thermocouple placed in close contact with the cuvette. The wire thermocouple (K-type) and meter (HH-51) were obtained from Omega (Stamford, CT).

REFERENCES

(1) Lee, J.C. Thesis, California Institute of Technology, 2002.

(2) Banci, L.; Bertini, I.; Huber, J.G.; Spyroulias, G.A.; Turano, P. Solution Structure of Reduced Horse Heart Cytochrome *c*. *J. Biol. Inorg. Ch*em. **1999**, *4*, 21-31.

(3) Anni, H.; Vanderkooi, J.M.; Mayne, L.C.; Structure of Zinc-substituted Cytochrome *c*-Nuclear Magnetic Resonance and Optical Spectroscopic Studies. *Biochemistr*y **1995**, *34*, 5744-5753.

(4) Finkelstein, A.V. Shakhnovich, E.I. Theory of Cooperative Transitions in Protein Molecules. *Biopolymers* **1989**, *28*, 1681-1694.

(5) Garcia, A.E.; Hummer, G. Water Penetration and Escape in Proteins. *Proteins* **2000**, *38*, 261-272.

(6) Otting, G.; Liepinsh, E.; Wuthrich, K. Protein Hydration in Aqueous Solution. *Science* **1991**, *254*, 974-980.

(7) Ernst, J.A.; Clubb, R,T; Zhou, H.X.; Gronenborn, A.M.; Clore, G.M. Demonstration of Positively Disordered Water Within a Protein Hydrophobic Cavity by NMR. *Science* **1995**, *267*, 1813-1817.

(8) Fernandez-Escamilla, A.M.; Cheung, M.S.; Vega, M.C.; Wilmanns, M.; Onuchic, J.N.; Serrano,L. Solvation in protein folding analysis: Combination of theoretical and experimental approaches. *Proc. Natl. Acad. Sci. U.S.A.* **2004**, *101*, 2834-2839.

(9) Sudha, B.P.; Dixit, S.N.; Moy, V.T.; Vanderkooi, J.M. Reaction of Excited-state Cytochrome c Derivatives- Delayed Fluorescence and Phosphorescence of Zinc, Tin, and Metal-free Cytochrome *c* at Room Temperature. *Biochemistr*y **1984**, *23*, 2103-2107.

(10) Voet, D.; Voet, J.; Pratt, C.W. *Fundamentals of Biochemistry*. Wiley: New York, 1999.

(11) Course 5.48J, Protein Folding Problem, MIT OpenCourseWare,

http://ocw.mit.edu/OcwWeb/Biology/7-88JProtein-Folding-ProblemFall2003/CourseHome/index.htm

(12) Elias, H.; Chou, M; Winkler, J.R. Electron-Transfer Kinetics of Zn-substituted Cytochrome *c* and Its $Ru(NH_3)_5$(Histidine-33) Derivative. *J. Am. Chem. Soc*. **1988**, *110*, 429-434.

(13) Seksek, O.; Biwersi, J.; Verkman, A.S. Translational Diffusion of Macromolecule-sized Solutes in Cytoplasm and Nucleus. *J. Cell Bio.* **1997**, *138*, 131-142.

(14) Luby-Phelps, K.; Castle, P.E.; Taylor, D.L.; Lannin, F. Hindered Diffusion of Inert Tracer Particles in the Cytoplasm of Mouse 3T3 Cells. *Proc. Natl. Acad. Sci. U.S.A.* 1987, *84*, 4910-4913.

(15) Potma, E.O.; Boeij, W.P.; Bosgraaf, L.; Roelofs, J.; van Haastert, P.J.; Wiersma, D.A. Reduced Protein Diffusion Rate by Cytoskeleton in Vegetative and Polarized Dictyostelium Cells. *Biophys. Journal* **2001**, *81*, 2010-2019.

(16) Ovadi, J.; Saks, V. On the Origin of Intracellular Compartmentation and Organized Metabolic Systems. *Mol. and Cell. Biochem.* **2004**, *256*, 5-12.

(17) http://www.exploratorium.edu/traits/images/ecoli_drawn.jpg

(18) http://www.bgu.ac.il/~aflaloc/images/crowdedBact.jpg

(19) Ellis, J.R. Macromolecular Crowding: Obvious but Underappreciated. *TRENDS in Biochem. Sciences* **2001**, *26*, 597-604.

(20) Ellis, J.R.; Minton, A.P. Cell Biology - Join the Crowd. *Nature* **2003**, *425*, 27-28.

(21) Hall, D..; Minton, A.P. Macromolecular Crowding: Qualitative and Semiquantitative Successes, Quantitative Challenges. *Biochimica et Biophysica Acta* **2003**, *1649*, 127-139.

(22) Mukherjee, S.; Waegele, M.M.;, Chowshury, P.; Guo, L.; Gai, F. Effect of Macromolecular Crowding on Protein Folding Dynamics at the Secondary Structure

Level. *J. Mol. Bio.* **2009,** *393*, 227-236.

(23) Eggers, D.K.; Valentine, J.S. Molecular Confinement Influences Protein Structure and Enhances Thermal Protein Stability. *PROTEIN SCIENCE* **2001**, *10*, 250-261.

(24) van den Berg, B.; Ellis, R.J.; Dobson, C.M. Effects of Macromolecular Crowding on Protein Folding and Aggregation. *EMBO J.* **1999**, *18*, 6927-6933.

(25) Eggers, D.K.; Valentine, J.S. Crowding and Hydration Effects on Protein Conformation: A Study with Sol-gel Encapsulated Proteins. *J. Mol. Bio.* **2001**, *314*, 911-922.

(26) Weiss M, Elsner M, Kartberg F, et al. Anomalous Subdiffusion is a Measure for Cytoplasmic Crowding in Living Cells. *Biophys. J.* **2004**, *87*, 3518-3524.

(27) Cheung, M.S.; Klimov, D.; Thirumalai, D. Molecular Crowding Enhances Native State Stability and Refolding Rates of Globular Proteins *Proc. Natl. Acad. Sci U.S.A* **2005**, 102, 4753-4758.

(28) van den Berg, B.; Wain R, Dobson C.M.; et al. Macromolecular Crowding Perturbs Protein Refolding Kinetics: Implications for Folding Inside the Cell. *EMBO J.* **2000**, *19*, 3870-3875.

(29) Martin, J.; Hartl, F.U. The Effect of Macromolecular Crowding on Chaperonin-Mediated Protein Folding. *Proc. Natl. Acad. Sci U.S.A.* **1997**, 94, 1107-1112.

(30) Hall, D. Protein Self-association in the Cell: a Mechanism for Fine Tuning the Level of Macromolecular Crowding? *Eur. Biophys. J.* **2006**, *35*, 276-280.

(31) Batra, J.; Xu, K.; Zhou, H.X. Nonadditive Effects of Mixed Crowding on Protein Stability. *PROTEINS* **2009**, *77,* 133-138.

(32) Kulothungan, S.R.; Das, M.; Johnson, M.; et al. Effect of Crowding Agents, Signal Peptide, and Chaperone SecB on the Folding and Aggregation of E. coli Maltose Binding Protein. *Langmuir* **2009**, *25*, 6637-6648.

(33) Munishkina, L.A.; Fink, A.L.; Uversky, V.N. Accelerated Fibrillation of alpha-Synuclein Induced by the Combined Action of Macromolecular Crowding and Factors Inducing Partial Folding. *Curr. Alzheimer Res.* **2009**, *6*, 252-260.

(34) Homouz, D.; Stagg, L.; Wittung-Stafshede, P.; et al. Macromolecular Crowding Modulates Folding Mechanism of alpha/beta Protein Apoflavodoxin. *Biophys. J.* **2009**, *96*, 671-680.

(35) Samiotakis, A.; Wittung-Stafshede, P.; Cheung, M.S. Folding, Stability and Shape of Proteins in Crowded Environments: Experimental and Computational Approaches. *Int. J. Mol. Sci.* **2009**, *10*, 572-588.

(36) Mittal, J.; Best, R.B. Thermodynamics and Kinetics of Protein Folding Under Confinement. *Proc.Natl. Acad. Sci U.S.A.*. **2008**, *105*, 20233-20238.

(37) Homouz, D.; Perham, M.; Samiotakis, A.; et al. Crowded, Cell-like Environment Induces Shape Changes in Aspherical Protein. *Proc. Natl. Acad. Sci U.S.A.*. **2008**, *105*, 11754-11759.

(38) Zhou, H.X.; Rivas, G.N.; Minton, A.P. Macromolecular Crowding and Confinement: Biochemical, Biophysical, and Potential Physiological Consequences. *Annu. Rev. Biophys.* **2008**, *37*, 375-397.

(39) Charlton, L.M.; Barnes, C.O.; Li, C.G.; et al. Residue-level Interrogation of Macromolecular Crowding Effects on Protein Stability. *J. Am. Chem. Soc.* **2008**, *130*, 6826-6830.

(40) Konopka, M.C.; Weisshaar, J.C.; Record, M.T. Methods of Changing Biopolymer Volume Fraction and Cytoplasmic Solute Concentrations for *in vivo* Biophysical Studies.
Methods Enzymol. **2007**, *428*, 487-504.

(41) Cheung, M.S.; Thirumalai, D. Effects of Crowding and Confinement on the Structures of the Transition State Ensemble in Proteins. *J. Phys. Chem. B* **2007**, *111*, 8250-8257.

(42) Hall, D.; Dobson, C.M. Expanding to Fill the Gap: A Possible Role for Inert Biopolymers in Regulating the Extent of the 'Macromolecular Crowding' Effect. *FEBS Lett.* **2006**, *580*, 2584-2590.

(43) Hall, D. Protein Self-association in the Cell: a Mechanism for Fine Tuning the Level of Macromolecular Crowding. *Eur. Biophys. J.* **2006**, *35*, 276-280.

(44) Martinez-Haya, B.; Gordillo, A.C. Effect of Macromolecular Crowding on the Conformation of Confined Chain Polymers. *Macromol. Theory Simul.* **2005**, *14*, 421-427.

(45) Minton, A.P. Influence of Macromolecular Crowding Upon the Stability and State of Association of Proteins: Predictions and observations. *J. Pharm. Sci.* **2005**, *94*, 1668-1675.

(46) Spencer, D.S.; Xu, K.; Logan, T.M.; et al. Effects of pH, Salt, and Macromolecular Crowding on the Stability of FK506-binding Protein: An Integrated Experimental and Theoretical Study. *J. Mol. Bio.* **2005**, *351*, 219-232.

(47) Lukacs, G.L.; Haggie, P.; Seksek, O.; Lechardeur, D.; Freedman, N.; Verkman, A.S. Size-dependent DNA Mobility in Cytoplasm and Nucleus. *J. Bio. Chem.* **2000**, *275*, 1625-1629.